Journal of proteome research

Article

pubs.acs.org/jpr

Comparative Glycoproteome Analysis: Dynamics of Protein Glycosylation during Metamorphic Transition from Pelagic to Benthic Life Stages in Three Invertebrates

Kondethimmanahalli H. Chandramouli, Yu Zhang, Yue Him Wong, and Pei-Yuan Qian*

KAUST Global Collaborative Research Program, Division of Life Science, Hong Kong University of Science and Technology, Hong Kong SAR, China

ABSTRACT: The life cycle of most benthic marine invertebrates has two distinct stages: the pelagic larval stage and the sessile juvenile stage. The transition between the larval stage and the juvenile stage is often abrupt and may be triggered by post-translational modification of proteins. Glycosylation, a very important post-translational modification, influences the biological activity of proteins. We used two-dimensional gel electrophoresis (2-DE) followed by glycoprotein-specific fluorescence staining and mass spectrometry with the goal of identifying glycosylation pattern changes during larval settlement and metamorphosis in barnacles, bryozoans, and polychaetes. Our results revealed substantial changes in the protein glycosylation patterns from larval to juvenile stages. Before metamorphosis, the degree of protein glycosylation was high in the barnacle *Balanus* (=*Amphibalanus*) *amphitrite* and the spionid polychaete *Pseudopolydora vexillosa*, whereas it increased after metamorphosis in the bryozoan *Bugula neritina*. We identified 19 abundant and differentially glycosylated proteins in these three species. Among the proteins, cellular stress- and metabolism-related proteins exhibited distinct glycosylation in *B. amphitrite* and *B. neritina*, whereas fatty acid metabolism-related proteins were abundantly glycosylated in *P. vexillosa*. Furthermore, the protein and gene expression analysis of some selected glycoproteins revealed that the degree of protein glycosylation did not always complement with transcriptional and translational changes associated with the larval–juvenile transition. The current study provides preliminary information on protein glycosylation in marine invertebrates that will serve as a solid basis for future comprehensive analysis of glycobiology during larval settlement and metamorphosis.

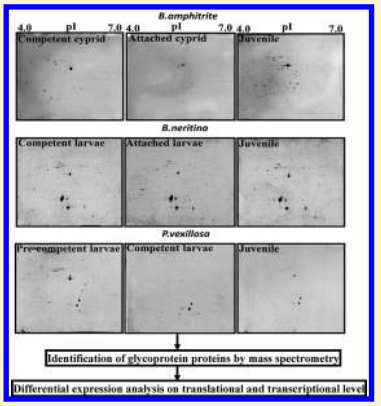

KEYWORDS: *2-DE, glycoproteomics, marine invertebrates, larval metamorphosis, transcription, translation*

INTRODUCTION

Most benthic marine invertebrates have a microscopic, planktonic larval phase during their complex life cycles. Many factors, such as settlement cues, the timing of larval release, the timing of metamorphosis initiation, and the extent of morphological changes, influence larval settlement and metamorphosis. On the basis of these factors, larvae may spend minutes, weeks, or even months in the water column before they attain competence to attach and metamorphose.[1,2] In some invertebrates, the developmental capacity to settle occurs within hours after fertilization, whereas other species require a significantly longer period before attaining competence to metamorphose.[3−6] The transition between the pelagic larval and benthic juvenile stages of these species is often abrupt and involves morphological, physiological, and functional changes mediated by differential expression and post-translational modification (PTM) of proteins.[7] For instance, larval settlement of the barnacle *Balanus amphitrite* is a dynamic and rapid process involving substantial tissue differentiation.[8] Under controlled laboratory conditions, the larva–juvenile transition of barnacles may or may not require a metamorphosis inducer.[9] Mature bryozoan *Bugula neritina* directly release competent larvae into the water column that often settle within a few minutes without any cues.[10,11] In contrast, the polychaete *Pseudopolydora vexillosa* releases young larvae into the water column. These larvae may take 7−10 days to attain competence to settle, and their metamorphosis is a gradual process and does not require substantial development of juvenile organs.[12] On the other hand, other marine invertebrates share common metamorphic transitions, including the loss of larval structures, habitat selection, and differentiation of juvenile/adult structures.[13] The molecular mechanisms regulating the larval–juvenile transition among these organisms that have contrasting larval development and settlement processes remain unidentified.

In many higher organisms, glycosylation of proteins modulates various processes such as subcellular localization, cell-to-cell recognition, and cell–matrix binding events.[14] In turn, these important functions control developmental processes such as morphogenesis or organogenesis.[15−19] In this study, we hypothesized that (1) interspecific differences in protein glycosylation attribute to differences in the developmental process during larval metamorphosis and (2) common protein glycosylation processes in different species may be involved in regulating larval metamorphosis. To test our

Received: September 30, 2011
Published: November 24, 2011

dx.doi.org/10.1021/pr200982k | *J. Proteome Res.* 2012, 11, 1330–1340

hypotheses, we used 2-DE technology followed by fluorescence-based staining to detect glycoproteins and to identify differing and common glycosylation proteins during three developmental stages in three marine invertebrates: the barnacle *B. amphitrite*, the bryozoan *B. neritina,* and the polychaete *P. vexillosa*.

EXPERIMENTAL SECTION

Selection of Larval Species and Larval Culture

The barnacle *Balanus amphitrite,* the bryozoan *Bugula neritina*, and the polychaete *Pseudopolydora vexillosa* were selected for this study. Large brood stocks of each species were collected from the field during the peak reproductive season (see below). Adult *B. amphitrite* were collected from the concrete columns of the pier at Pak Sha Wan in Hong Kong (22°21′45″ N, 114°15′35″ E), and the released naupliar larvae were reared to the cyprid stage following Thiyagarajan et al.[20,21] The nauplii developed into cyprids (CC) on day 4, and some were allowed to settle for 12 h in Petri dishes and were called attached cyprids (AC). To collect juveniles (JU), we allowed competent cyprids to attach and metamorphose in glass Petri dishes for 24 h. Larvae from each developmental stage as described above were transferred to lysis buffer (7 M of urea, 2 M of thiourea, 4% CHAPS, 1% DTT) and fixed for 2-DE.

Adult *B. neritina* were collected from the floating rafts of a fish farm in San Shing Wan, Hong Kong (22°21′19″ N, 114°16′15″ E) between February and April, 2010. Sexually mature *B. neritina* colonies were placed in a 10 L glass tank filled with seawater under bright artificial light to induce the release of larvae from the brood chambers of adult colonies. Competent swimming larvae (CL) were carefully selected under a dissecting microscope and were immediately transferred to lysis buffer and used for 2-DE as described by Wong et al.[22] A portion of the swimming larvae was placed in filtered seawater and allowed to settle (AL) for 4 h. To collect juveniles (JU), we allowed competent swimming larvae to metamorphose for 48−52 h and then transferred them to lysis buffer.

Adult spionid *P. vexillosa* were collected from the subtidal soft-bottom substrate in Sai Kung, Hong Kong (22°25′ N, 114°17′ E) and kept in the laboratory as brood stock. Precompetent (PC), competent (CL), and juveniles (JU) were collected for experiments by following the protocol described by Mok et al.[12]

Two-Dimensional Gel Electrophoresis

Sample preparation for two-dimensional gel electrophoresis (2-DE) was carried out as described by Chandramouli et al.[23] with slight modification. Briefly, the protein samples were purified using a 2-DE cleanup kit (Bio-Rad, Hercules, CA). The purified protein pellets were resolubilized in rehydration buffer (7 M of urea, 2 M of thiourea, 4% CHAPS, 1% DTT, 0.5% pH 4−7 ampholytes), and the protein concentration was determined using a modified Bradford method.[24] For each protein sample, 300 μg were sonicated for 10 min on ice and incubated at room temperature (∼24 °C) for 2 h to enhance protein solubilization. After rehydration of protein sample on 17 cm, pH 4−7 linear IPG strips for 14−16 h, proteins were then subjected to isoelectric focusing (IEF) using a Protean IEF Cell (Bio-Rad, Hercules, CA).

Focusing was carried out at 250 V for 20 min and then along a gradient from 1000 to 8500 V to give a total of 60 000 voltage-hr. After IEF, consecutive reduction and alkylation of the IPG strips were carried out using 2% DTT and 2.5% iodoacetamide (IAA) respectively in an equilibration buffer (6 M urea, 2% sodium dodecyl sulfate [SDS], 0.05 M Tris-HCl [pH 8.8], 50% glycerol, 2% [w/v] DTT). The second dimension was performed on 12% polyacrylamide SDS-PAGE gels using Protean II Multicell (Bio-Rad, Hercules, CA) following the protocol described by Zhang et al.[25]

Gel Staining and Image Analysis

2-DE gels were stained for glycoproteins using the Pro-Q Emerald 488 glycoprotein gel stain kit (Invitrogen, Eugene, OR) according to the manufacturer's instructions. Briefly, gels were fixed overnight in 40% methanol and 10% acetic acid and then incubated in an oxidizing solution for 1 h. After being washed with 3% acetic acid, the gels were incubated in a Pro-Q Emerald 488 dye solution for 90 min. The gels were again washed with 3% acetic acid before scanning. The glycoprotein spots were visualized by a Typhoon trio imager (GE Healthcare, Piscataway, NJ) at an excitation of 488 nm with a 520 nm BP emission filter. After detection of glycoproteins, the gels were stained by SYPRO Ruby protein gel stain overnight in the dark and scanned using the Typhoon trio imager at an excitation of 582 nm with a 610 BP 30 emission filter (data not shown). Three replicate gels for glycoproteins were quantitatively and qualitatively analyzed using the PDQuest software (Bio-Rad, Hercules, CA) as described by Thiyagarajan et al.[26] The glycosylation level of each protein spot was normalized by the total protein expression level. A 1.5-fold threshold was set for quantitative detection of the spot intensity of the glycoproteins in three developmental stages. Glycoprotein spots that were significantly different (Student's *t*-test, $p < 0.05$) in successive stages were considered to be up- or down-regulated.

Identification of Glycoproteins by Mass Spectrometry

MALDI-TOF/TOF Analysis. The 2-DE gels were post-stained with Coomassie brilliant blue G-250. The reproducible and abundant glycoprotein spots were excised, and digested in 20 μL of 12.5 ng/mL trypsin (Promega, Madison, WI) in 10% acetonitrile and 10 mM of NH_4HCO_3 at 37 °C for 16 h. The peptides were extracted and dried in a speed vacuum following the protocol described by Qian et al.[27] The samples were analyzed using an Autoflex III TOF/TOF mass spectrometer (Bruker Daltonics, Bellirica, MA). Mass spectra were acquired in positive reflector mode, using an acceleration voltage of 20 kV and a delayed extraction of 80 ns. Spectra were recorded from 500 to 3500 m/z units, each spectrum corresponding to a minimum of 300 laser shots. The MS and MS/MS spectra were combined using the BioTools software (version 3.1, Bruker Daltonics) and searched against the in-house transcriptome databases of *B.amphitrite*, *B. neritina*, and *P. vexillosa* using the MASCOT software (Matrix Science). The MS spectra were also searched against the NCBI nr database to identify the proteins already listed in transcriptome databases. The search parameters were set at 50 ppm for peptide tolerance and 0.2 Da for MS/MS tolerance, oxidation at methionine and phosphorylation at serine, threonine, as variable modifications. Carboxamidomethylation at cysteine residues was set as a fixed modification. Search results from the combined spectra that were statistically significant ($p < 0.05$) were considered to be positive identifications.

ESI-QTOF Analysis. Each of the dried peptide samples was reconstituted in 10 μL of 0.1% formic acid. The peptides were desalted using C18 ZipTip (Millipore, Billerica, MA) and then

dx.doi.org/10.1021/pr200982k | J. Proteome Res. 2012, 11, 1330−1340

analyzed using a nanoflow UPLC (nanoAcquity, Waters) coupled with an ESI-hybrid Q-TOF tandem mass spectrometer (Premier, Waters). The Q-TOF was set to perform data-dependent acquisition in the positive ion mode with a selected MS survey mass range of 300−1600 m/z. The three most abundant peptides with +2 to +4 charge states above a 40-count threshold were selected for MS/MS as described by Zhang et al.[28] The MS raw data were searched against a corresponding customized in-house transcriptome database. The mass tolerances were set at 30 ppm for the peptide precursors and 0.5 Da for the fragment ions. Carboxamidomethylation at cysteine residues was set as a fixed modification, and oxidation at methionine as well as phosphorylation at serine, threonine, or tyrosine were set as variable modifications.

SDS-PAGE and Western Blot Analysis

We also compared the corresponding protein expression levels of four selected glycoproteins (hsp-90, 14-3-3, tubulin, actin) by Western blot analysis following the protocol described by Zhang et al.[29] Briefly, 20 μg of protein lysates from *B. amphitrite* (CC, AC, and JU stages) and *P. vexillosa* (PC, CL, and JU stages) were separated on 10% SDS-PAGE and transferred onto Immobilon transfer membranes (Millipore, Billerica, MA). The membranes were incubated with 1:1000 diluted monoclonal antibodies of anti-tubulin, anti-actin, anti-hsp90 (Cell Signaling, Danvers, MA) and anti-14-3-3 antibodies (Abcam, Cambridge, MA) for ∼16 h at 4 °C. The membranes were then probed with horseradish peroxidase-conjugated secondary antibodies (1:5000 dilution) for 1 h at room temperature, followed by chemiluminescent detection using an ECL Western blotting analysis system (Millipore, Billerica, MA).

Semiquantitative Real-Time PCR

To gain more insight into the gene expression patterns of differentially glycosylated proteins, quantitative real-time PCR (qRT-PCR) was performed following the protocol detailed by Wong et al.[22] Briefly, total RNA of selected stages of two species (*B. amphitrite*: naupilus (NU), CC, and JU; *B. neritina*: CL, AL, and JU) was isolated using the TRIzol reagent (Invitrogen, Carlsbad, CA) according to the supplier's instructions. The extracted total RNA was digested with DNase (Turbo DNA-free Kit, Applied Biosystems, Carlsbad, CA) to remove trace DNA contaminants. The cDNA was synthesized from 2 μg of total RNA from each stage using M-MLV reverse transcriptase (USB, Cleveland, OH) with a random hexamer primer. Gene-specific primers were designed on the basis of the nucleotide sequence of the target protein in the respective transcriptome databases. 18S RNA and *Cytochrome b* genes were chosen as the reference genes to normalize the expression levels of the target genes in *B. neritina* and *B. amphitrite*, respectively. qRT-PCR assays for each target gene were performed in triplicate and repeated twice. All qRT-PCR assays were carried out using iTaq SYBR Green Supermix with ROX (Bio-Rad, Foster City, CA) and run on the 7500 Fast Real-Time PCR System (Applied Biosystems, Foster City, CA). The qRT-PCR data were analyzed by the 2-ΔΔCT method as described by Livak and Schmittgen.[30]

RESULTS

Glycosylation Patterns of Different Developmental Stages in Three Species

The glycoprotein profiles of three developmental stages of *B. amphitrite*, *B. neritina*, and *P. vexillosa* are shown in Figure 1A−C.

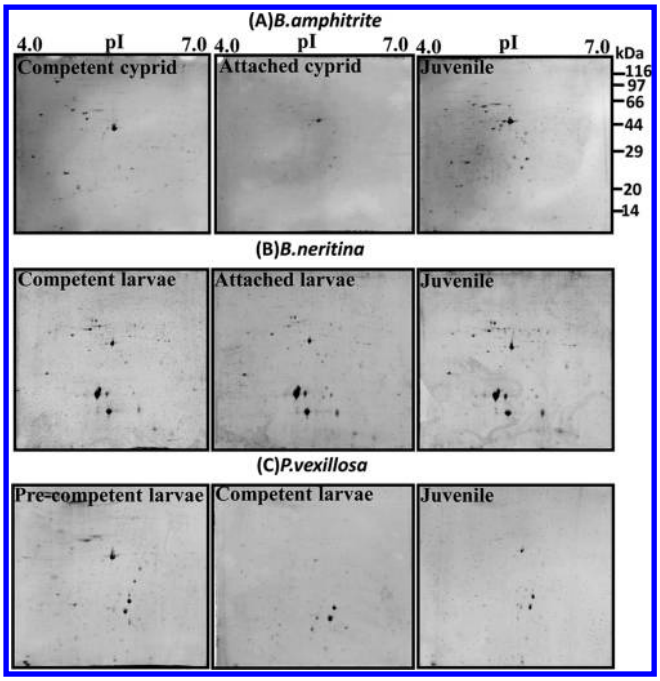

Figure 1. A representative glycoprotein profile obtained from three developmental stages of three species. Proteins were separated on 17 cm, pH 4−7 linear IPG strips in the first dimension, and the second dimension was performed on a 12% polyacrylamide SDS-PAGE. The 2-DE gels were stained with Pro-Q Emerald 488 dye for glycoprotein detection.

The analysis of three independent replicate gels from three developmental stages of each species revealed that significant differences in glycosylation existed in some glycoproteins ($P < 0.05$). In *B. amphitrite*, 45, 22, and 28 ($n = 3$) glycoprotein spots were detected from the CC, AC, and JU stages, respectively (Figure 2A). In *B. neritina*, 23, 32, and 45 ($n = 3$) glycoprotein spots were detected from the CL, AL, and JU stages, respectively (Figure 2B), whereas in *P. vexillosa*, 29, 11, and 6 ($n = 3$) glycoprotein spots were detected from the PC, CL, and JU stages, respectively (Figure 2C). After glycoprotein staining, the 2-DE gels were subsequently stained with SYPRO Ruby, which were used as reference gels to compare protein expression patterns in the same gels (data not shown). The 2-DE maps revealed that the pattern of protein glycosylation changed substantially from the larval to juvenile stages in all three species. More glycoprotein spots were detected in the CC stage than in the AC and JU stages (Figure 2A) in *B. amphitrite*. In contrast, the CL stage of *B. neritina* had fewer glycoprotein spots than the AL and JU stages, whereas in *P. vexillosa*, the glycoprotein spots drastically decreased from the PC to JU stages.

Identification of Commonly Expressed Glycoproteins and Species-Specific Glycosylation of Proteins

In total, 41 glycoproteins were identified (Figure 3 and Table 1) from all three species. Notably, 11 glycoproteins (spots 1−11) were identified as commonly glycosylated proteins among the three developmental stages in *B. amphitrite* and *B. neritina*. Five glycoproteins (α-TUB, β-TUB, ACT, TM, and 14-3-3) were commonly glycosylated in the three developmental stages of the three species. Eight proteins exhibited species-specific glycosylation patterns across all three species. Calreticulin (CAL) (spot 12), cuticular protein 111(CP3) (spot 13), and translationally controlled tumor protein (TCTP) (spot 14)

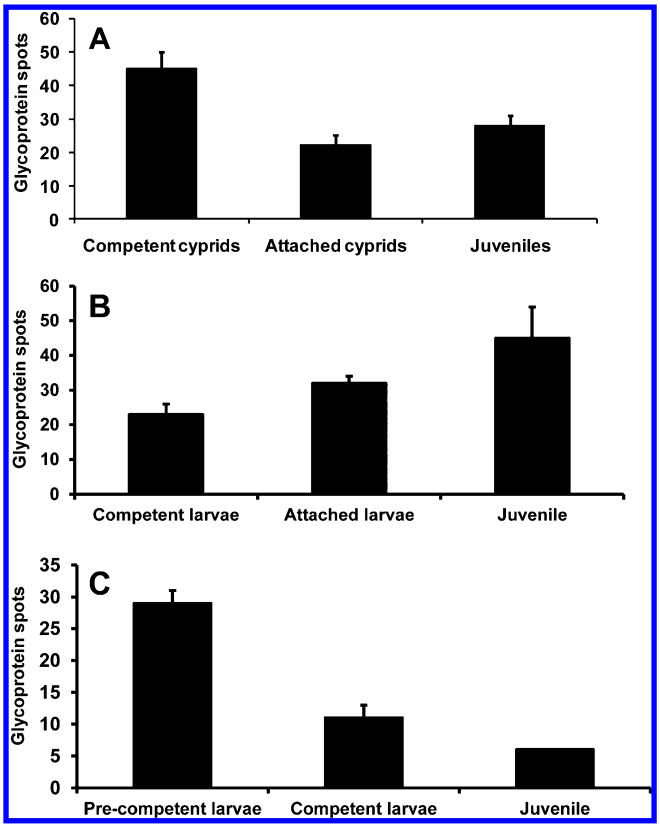

Figure 2. Changes in glycosylation pattern during larval settlement and metamorphosis. The number of glycoprotein spots reproducibly detected in three developmental stages. (A) *B. amphitrite*, (B) *B. neritina*, and (C) *P. vexillosa*.

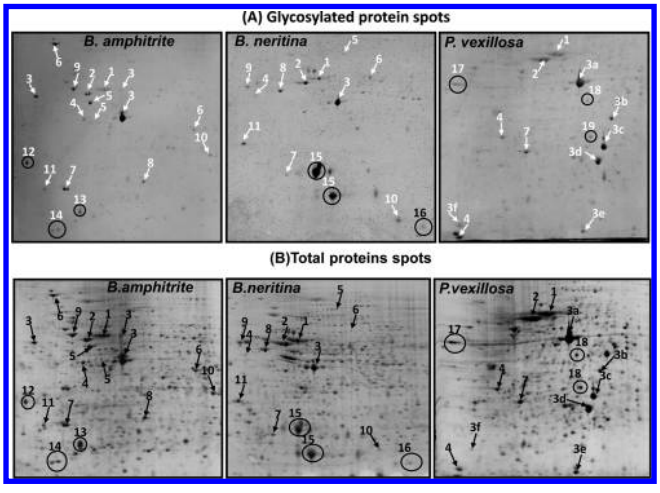

Figure 3. A Pro-Q Emerald 488 glycoprotein 2-D gel (A) showing glycosylated protein spots that were differentially glycosylated (marked with an arrow) or abundant protein spots with species-specific glycosylation (marked with circles). 2-D gel (B) showing total protein spots that were differentially glycosylated or showed species-specific glycosylation. Spot numbers correspond to those listed in Table 1. (left) Competent cyprid of *B. amphitrite*, (middle) competent larvae of *B. neritina*, and (right) precompetent larvae of *P. vexillosa*.

exhibited specific glycosylation in *B. amphitrite* (Figure 3; *B. amphitrite*, spots marked with circles), whereas in *B. neritina*, vitellogenin-6 (VTG 6) (spot 15) and galactose mutarotase (GALM) (spot 16) were specifically glycosylated (Figure 3: *B. neritina*, spots marked with circles). Enolase-phosphatase E1 (EP1) (spot 17), cytoplasmic intermediate filament (CIF) (spot 18), and low-density lipoprotein receptor (LDLR) (spot 19) exhibited specific glycosylation in *P. vexillosa* (Figure 3: *P. vexillosa*, spots marked with circles). Total protein expression of these proteins is shown in Figure 3, lower panel.

The Dynamics of Protein Glycosylation during Larval Development and Metamorphosis

Cytoskeleton proteins exhibited differing glycosylation patterns in the three species (Figure 3, Table 1, spots 1−3). Specifically, oxidative stress- and energy metabolism-related proteins (Table 1, spots 5−11, 15, and 16) revealed distinct glycosylation in *B. amphitrite* and *B. neritina*. In contrast, fatty acid metabolism-related proteins were abundantly glycosylated in *P. vexillosa* (Figure 3: *P. vexillosa*, Table 1, spots 17 and 19). Interestingly, several glycoprotein spots were identified as the same protein or isoforms of the same protein, such as actin (ACT) in *P. vexillosa* (Figure 3: *P. vexillosa*, Table 1, spots 3a−f). In *B. amphitrite*, TM, hsp90, PDI, MDH, CAL, and CP3 exhibited higher glycosylation in the CC stage, and the glycosylation levels of these proteins gradually decreased in the AC and JU stages. The 14-3-3, CP, and TCTP glycosylation levels drastically decreased in the AC stage but were sustained at the same level in JU stage. In *B. neritina*, α-TUB and β-TUB exhibited decreased glycosylation in the AL stage, and the level was sustained in the JU stage. In contrast, VTG 6 glycosylation decreased in the JU stage. ATPsyn-β, TM, CP, and MDH exhibited decreased glycosylation in the JU stage. In *P. vexillosa*, α-TUB, β-TUB, ACT, LDLR, and 14-3-3 exhibited decreased glycosylation in the CL and JU stages. TM and CIF exhibited species-specific glycosylation in the PC stage.

To determine whether these variations in glycosylation among the three species were due to changes in the total protein expression, we compared the total protein expression of the glycosylated proteins on the same gels. In *B. amphitrite*, changes in the glycosylation of Hsp90, MDH, CAL, PDI, 14-3-3, TCTP, and CP were merely due to their protein expression changes (Figure 3 and Table 1; *B. amphitrite*). Similarly, in *B. neritina*, the decrease of tubulin glycosylation in the AL stage and its subsequent increase in the JU stage was due to total protein expression changes (Figure 3 and Table 1; *B. neritina*).

Differentially Glycosylated Proteins at Translational and Transcriptional Levels

To date, antibodies against proteins/glycoproteins are not commercially available for all of the tested species. Therefore, we chose four conserved proteins (hsp-90, 14-3-3, TUB, ACT) to test their total protein expression levels in three developmental stages of *B. amphitrite* and *P. vexillosa*. In *B. amphitrite*, hsp 90 expression was higher in the CC stage but gradually decreased from the AC to the JU stage (Figure 4A). Another glycoprotein, 14-3-3, was down-regulated in the AC stage but the expression was sustained in the JU stage (Figure 4B). These changes in protein expression (hsp-90 and 14-3-3) levels were consistent with the expression levels detected by Sypro Ruby, and their respective glycosylation levels also complemented the proteomics results. In *P. vexillosa*, expression of TUB and ACT was up-regulated in the CL stage and was slightly different in the JU stage (Figure 4C and D). Interestingly, we observed the opposite trend in the glycosylation variation in comparison with the proteomics study in which degree of glycosylation drastically decreased

dx.doi.org/10.1021/pr200982k | *J. Proteome Res.* 2012, 11, 1330−1340

Table 1. Identification of Glycosylated Proteins by MALDI-TOF and ESI-QTOF[a]

spot number	contig/NCBI nr access numbers	protein name	MW (kDa) obs/theor	pI obs/theor	PM/SC (%)	glycosylation/total protein variation ratios		
		B. amphitrite				CC	AC	JU
1	gil116740271	alpha-tubulin	43/43	6.9/5.9	10/18	1.4	1.4	1.4
						1.5	0.4	1.3
2	Contig807_27/gil78190577	beta-tubulin	55/43	5.3/5.7	11/37	1.4	1.4	1.6
						1.2	0.5	1.5
3	Contig02205/gil37528876	actin	50/41	4.3/5.5	11/43	1.9	1.9	1.9
						1.7	1.9	2.0
4[b]	adultGBQDZ6L01CGYE710/gil 290908989	myosin light chain	12/17	4.6/4.6	3/8	1.6	1.2	1.2
						1.6	1.3	1.5
5[b]	Contig28454_23/gil29468050	HSP-70	60/70	4.4/5.3	11/13	1.6	1.5	1.5
						1.6	0.4	1.0
6	gil32967463	HSP-90	40/83	4.8/5.1	5/18	1.4	0	0
						1.4	0.4	0.2
07[b]	Contig11093_23/gil161898814	14-3-3 zeta	29/28	4.7/4.8	12/20	1.5	1.0	1.5
						1.6	0.5	1.2
8	Isotig08551/gil46909259	ATP synthase beta subunit	46/50	5.0/4.8	3/32	1.6	1.6	1.3
						1.1	0.3	1.7
9[b]	Contig3516_16/gil170056920	disulfide isomerase	65/55	4.7/4.8	4/13	1.5	1.1	1.1
						1.4	1.0	0.9
10[b]	Contig14517_29/gil321457956	mitochondrial malate dehydrogenase	34/39	6.6/9.0	10/21	1.4	0.6	0.6
						1.3	0.5	0.6
11[b]	adultGBQDZ6L01BR/gil91992508	cathepsin L	29/38	4.4/5.7	2/9	1.4	0.8	1.4
						1.4	0.8	1.4
12	Isotig13155/gil47550939	calreticulin	49/53	4.2/4.8	6/18	1.4	1.1	1.1
						1.2	1.9	1.8
13[b]	nacF51RSDG03G13H4_11/gil 158286603	cuticular protein 111, RR-3 family	25/33	4.8/4.9	11/30	1.5	1.1	1.1
						1.5	1.0	1.3
14[b]	Contig5716_12/gil170034829	translationally controlled tumor protein	18/19	4.6/4.6	6/46	1.4	0.7	1.3
						1.3	0.7	1.2
		B. neritina				CL	AL	JU
1	Contig575_23/gil131573157	alpha-tubulin	51/55	4.9/5.2	7/3	1.6	1.0	1.5
						1.6	1.1	1.6
2[b]	Contig245_11/gil194068375	beta-tubulin	29/50	4.6/4.7	27/14	1.9	1.2	1.9
						1.6	1.0	1.4
3	Contig139_10/gil91078486	actin, cytoplasmic A3a	42/46	5.2/5.4	43/14	3.0	3.1	3.0
						3.0	1.5	3.1
4	Contig43_18	tropomyosin	34/29	4.6/4.5	23/7	0	1.0	1.5
						0	1.1	1.6
5	Contig805_3	HSP-70	75/71	5.3/5.0	5/15	0	1.1	1.1
						0	1.0	1.3
6	Contig6154_9/gil32967463	HSP-90	40/83	4.8/5.1	5/18	1.4	1.5	1.5
						1.3	1.7	1.4
7	Contig6360_4	14-3-3 protein	30/28	4.7/4.8	8/15	1.1	1.2	1.1
						1.3	1.0	1.2
8[b]	Contig2468_11/gil158524726	mitochondrial ATP synthase beta subunit	62/46	4.7/5.0	25/46	2.0	2.0	1.5
						2.0	0.8	1.8
9[b]	Contig6390_5/gil126697420	protein disulfide isomerase	65/55	4.4/4.5	23/64	3.6	3.5	3.6
						3.7	3.3	3.4
10	Contig288610	malate dehydrogenase	23/25	6.6/8.5	22/5	1.5	1.5	1.3
						1.5	0.3	1.4
11[b]	Contig3230_12/gil159792912	cathepsin L	38/37	4.3/4.8	7/21	2.2	2.2	1.6
						2.0	2.0	2.1
15[b]	Contig2966_28/gil324500481	vitellogenin-6	30/43	5.2/8.0	25/2	5.5	5.5	2.5
						5.5	3.2	2.7
16[b]	FZN7G6S01A63RT_4/gil294637415	galactose mutarotase	22/38	6.0/6.0	28/46	1.0	1.2	1.0
						0.9	0.3	1.2

dx.doi.org/10.1021/pr200982k | J. Proteome Res. 2012, 11, 1330–1340

Table 1. continued

spot number	contig/NCBI nr access numbers	protein name	MW (kDa) obs/theor	pI obs/ theor	PM/SC (%)	glycosylation/total protein variation ratios		
		P. vexillosa				PC	CL	JU
1	gil159400261	alpha-tubulin	60/47	5.3/5.2	5/18	1.4	0	0.6
						0.5	2.7	1.5
2	gil78190577	beta-tubulin	55/43	5.3/5.7	11/37	1.3	0	0.4
						0.5	2.6	1.6
3a	Contig56810077/gil37528876	actin, cytoplasmic A3	32/45	5.7/5.5	7/18	2.8	1.4	2.3
						0.7	2.7	1.5
3b[b]	Isotig01330_11/gil330858318	beta-actin	30/28	5.7/5.2	26/33	NA		
3c[b]	Isotig01330_11/gil330858318	beta-actin	30/28	5.7/5.6	26/33	NA		
3d[b]	F5K2Q4C01CF4OT_4/gil467215	actin	29/41	5.2/5.4	2/21	NA		
3e[b]	Isotig01887_4/gil330858318	beta-actin	18/28	4.2/5.2	15/45	NA		
3f[b]	isotig01330_11/gil330858318	beta-actin	14/28	5.3/5.2	27/45	NA		
4a	gil47117349	tropomyosin	35/39	4.5/4.6	8/19	NA		
4b[b]	Isotig00734_24/gil189007782	muscle myosin heavy chain	16/22	4.2/5.5	3/3	1.3	0	0
						2.0	6.3	0.2
7[b]	Isotig09326_6/gil315623847	14-3-3 zeta	29/16	4.7/4.6	2/7	1.3	0	0.4
						1.3	0	0.4
17	Contig08739_26/gil224049395	enolase-phosphatase E1	23/13	3.7/4.2	13/47	1.8	9.2	0.2
						1.7	9.2	0.2
18[b]	Isotig02676_13/gil4468655	cytoplasmic intermediate filament	42/68	5.4/5.6	1/3	1.3	0	0
						0.1	9.2	0.2
19[b]	Isotig04503_13/gil118093923	low-density lipoprotein receptor	32/17	5.5/5.1	13/17	1.2	0	1.2
						1.3	0	1.4

[a]Accession numbers are from the NCBI nr and corresponding in-house transcriptome databases. PM: number of peptides matching the protein sequence; SC: sequence coverage; CC: competent cyprids, AC: attached cyprids, JU: juvenile, CL: competent larvae, AL: attached larvae, PC: precompetent larvae. NA: not determined. [b]Glycoproteins identified by ESI-QTOF.

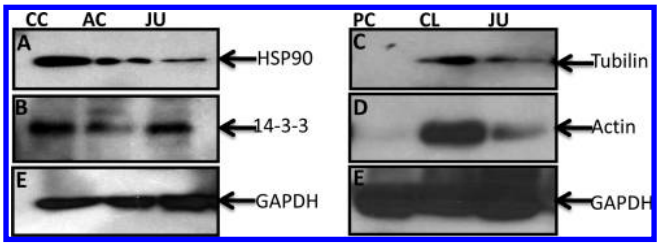

Figure 4. Western blot analysis of protein expression changes associated with larval settlement and metamorphosis in *B. amphitrite* (A: Hsp-90, B: 14-3-3) and *P. vexillosa* (C: Tubulin, D: Actin). Protein lysate (20 μg) was separated on a 10% SDS-PAGE gel. The membranes were incubated with corresponding monoclonal antibodies and developed by ECL Western blot analysis. GAPDH was used as a loading control (E).

from larval to juvenile stages (Table 1 and Figure 3, see *P. vexillosa* spots 1−3).

Genes encoding the selected glycoproteins from *B. amphitrite* and *B. neritina* (Table 2) were analyzed using semiquantitative RT-PCR. In *B. amphitrite*, TUB and hsp70 showed increased transcriptional expression in the JU stage (Figure 5A,B), whereas 14-3-3 exhibited increased expression in the CC stage and decreased expression in the JU stage (Figure 5C). ATPsyn-β and CAL showed no significant changes in the NU and CC stages, but expression decreased in the JU stage (Figure 5 D,E). Expression of ATPsyn-β and CAL correlated well with degree of glycosylation but differed from their total protein expression, whereas TUB, hsp-70, and 14-3-3 gene expression differed from their glycosylation levels but were parallel to the total protein expression in *B. amphitrite* (Figure 3 and Table 1; *B. amphitrite*). In *B. neritina*, the transcription of the cytoskeleton protein, TUB, was increased in the JU stage (Figure 6A), whereas gene expression of 14-3-3, TM, hsp90, and VTG drastically decreased in the JU stage (Figure 6C−F). VTG gene expression correlated well with the level of glycosylation. Hsp70 expression increased in AL when compared to CL and JU (Figure 6B). Notably, ATPsyn-β did not exhibit differential gene expression (data not shown).

DISCUSSION

Changes in Glycosylation Patterns Related to Interspecific Differences in Developmental Processes

This is the first comparative study demonstrating the changes in glycosylation patterns during larval settlement and metamorphosis in marine invertebrates. Changes in glycosylation patterns provide a snapshot of a dynamic glycoproteome at specific developmental stages. One of the major findings in this study is that protein glycosylation patterns changed markedly during larvae development in all three species analyzed. For instance, *B. amphitrite* and *P. vexillosa* larval proteins exhibited higher degrees of glycosylation before metamorphosis, whereas in *B. neritina*, the degree of glycosylation increased after metamorphosis. One explanation for these changes in glycosylation patterns may be related to interspecific differences attributed to varied developmental processes. For instance, the *B. amphitrite* life cycle includes six nauplius and one cyprid larval stages, and it would therefore likely require a longer time for *B. amphitrite* to attain competency to settle and metamorphose.[31] Before metamorphosis, the larvae participate in many complex activities, such as extensive searching for habitat selection with exposure to predation and environmental stresses.[32] Given these activities, the larvae may require high degrees of protein glycosylation in

dx.doi.org/10.1021/pr200982k | J. Proteome Res. 2012, 11, 1330−1340

Table 2. Gene Expression Analysis during Developmental Stages of *B. amphitrite* and *B. neritina*[a]

name of the gene	contig number	gene expression variation			primer sequence
B. amphitrite		NU	CC	JU	
tubulin	Isotig04752	1.0	1.0	1.3	FP: 5′-ACGCTGCACGTTCCCGATTT-3′
					RP: 5′-CCGTTCGGGTCAATGCCATGCT-3′
HSP-70	Isotig00187	1.0	1.2	1.5	FP: 5′-GGGCGAGGGACGGCGTTTAG-3′
					RP: 5′-CGGCGGTATGCCCGGAGGTA-3′
14-3-3	Isotig05524	1.0	1.8	1.0	FP: 5′-TTTGACGACCACCTCACATTCAACA-3′
					RP: 5′- TGCTGGGTCTCGCTGCAATCG-3′
ATP synthase beta subunit	Isotig08551	1.0	0.9	0.5	FP: 5′-GCCGCCGTTCTTGTCGGACA-3′
					RP: 5′-CAAGCAGGCGGTGGCCTACC-3′
calreticulin	Isotig13155	1.0	0.8	0.5	FP: 5′- TCGAGGCCCACCACACCGAT-3′
					RP: 5′-TGGAAGCCCCGCCAGATCGA-3′
B. neritina		CL	AL	JU	
tubulin	Contig607_23	1.0	2.3	7.9	FP: 5′-ACAGAGCCCTCACCGTCCCA-3′
					RP: 5′-TGGGATGTCACACACGGCGG-3′
HSP-70	Contig103_7	1.1	1.6	1.0	FP: 5′-TGGATGTGGCTCCACTGACCCT-3′
					RP: 5′TGGACACGGTAGTTTGCTGATCC-3′
14-3-3	Contig6360_4	1.3	3.0	1.5	FP: 5-GCTGGAGGCTACAGAGGAGCGT-3′
					RP: 5′-TGCGCCTCATTTGCCGACAACT-3′
ATP synthase beta subunit	Contig2226_7	1.1	1.1	1.1	FP: 5′-CCCTGCAGTACTTGGCCCCC-3′
					RP: 5′-AGCTTCACGACCTGGTGGACG-3′
tropomyosin	Contig47_18	1.0	1.2	0.2	FP: 5′-GCTGGAGGCTACAGAGGAGCGT-3′
					RP: 5′-TGCGCCTCATTTGCCGACAACT-3′
HSP-90	Contig6154_9	1.0	4.1	2.2	FP: 5′-CCTGACCCCGAGAACAAGACCCT-3′
					RP: 5′-CGGACCTGGCGATGGTACCG-3′
vitellogenin	Contig3144_28	1.1	2.0	0.2	FP: 5′-TCCCCATCTCCGTCTCTGCCC-3′
					RP: 5′-ACGAGTTGGGGCTCCCTGGT-3′

[a]NU: nauplius, CC: competent cyprid, JU: juvenile, CL: competent larvae, AL: attached larvae. FP: forward primer, RP: reverse primer.

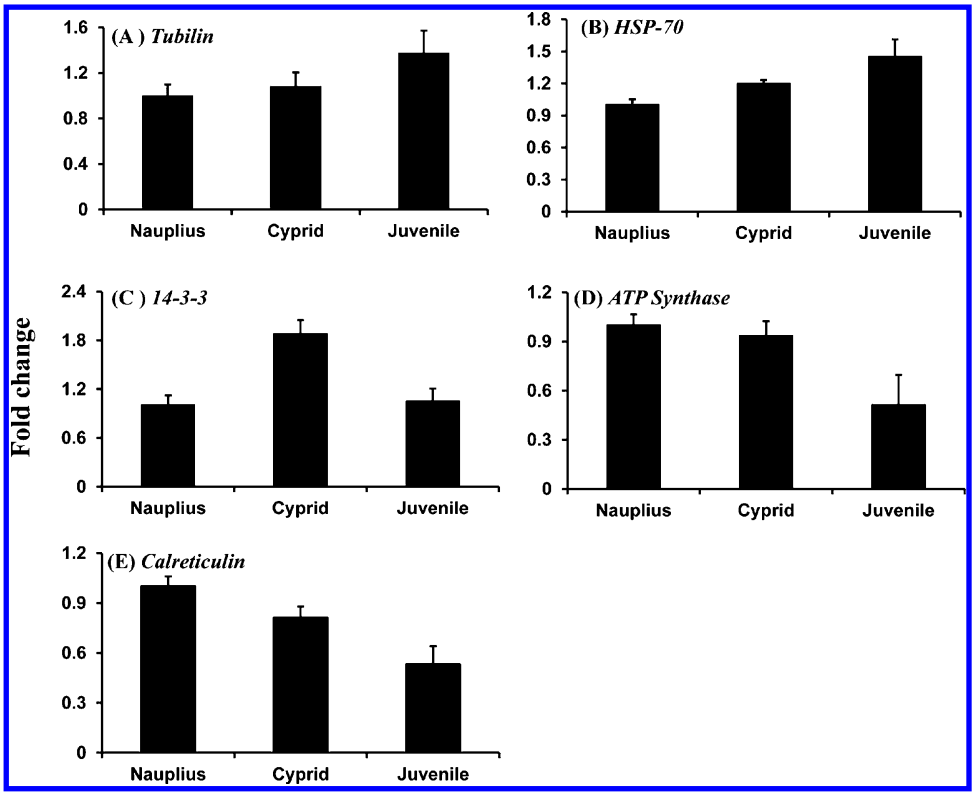

Figure 5. The gene expression pattern of (A) tubulin, (B) hsp-70, (C) 14-3-3, (D) ATP synthase, and (E) calreticulin during three developmental stages in *B. amphitrite*. Total RNA was isolated and cDNA was synthesized from 2 μg of total RNA from each stage. qRT-PCR assays for each target gene were performed in triplicate. The values are mean ± standard deviation obtained by normalization of target genes against reference genes.

dx.doi.org/10.1021/pr200982k | J. Proteome Res. 2012, 11, 1330–1340

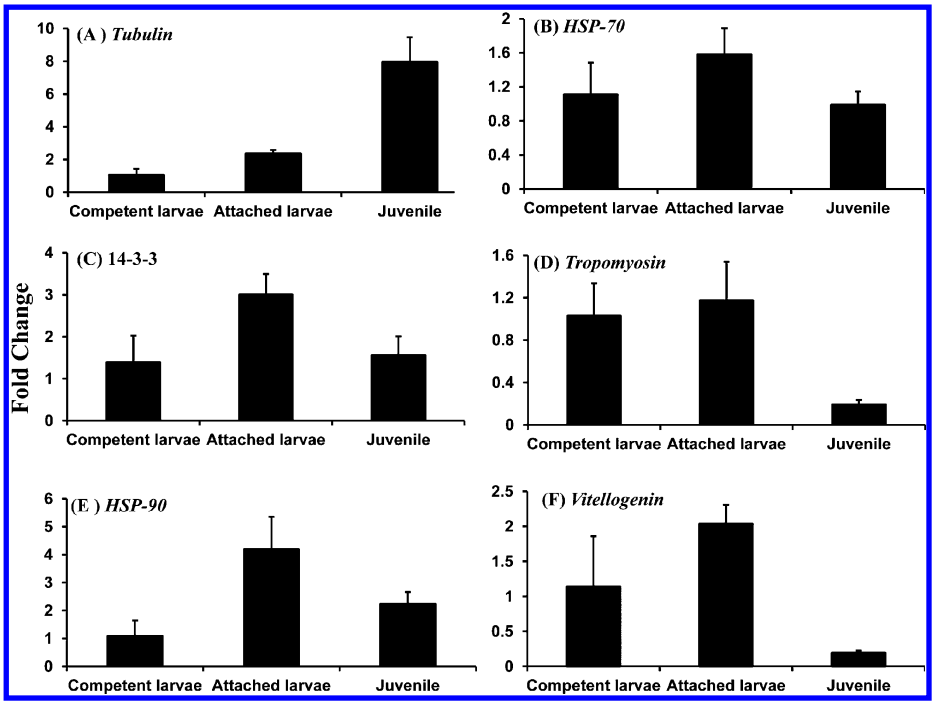

Figure 6. The gene expression profile of (A) tubulin, (B) hsp-70, (C) 14-3-3, (D) tropomyosin, (F) hsp-90, and (F) vitellogenin during three developmental stages in *B. neritina.* Total RNA was isolated and cDNA was synthesized from 2 μg of total RNA from each stage. qRT-PCR assays for each target gene were performed in triplicate. The values are mean ± standard deviation obtained by normalization of target genes against reference genes.

order to carry out these tasks. On the contrary, larval settlement and metamorphosis of the bryozoan *B. neritina* is relatively simple and rapid, and larvae may not require a high degree of protein glycosylation. After settlement, larvae then undergo substantial tissue differentiation and structural reorganization, which led to formation of juvenile tissues and organs. We suspect that *B. neritina* may require a higher degree of protein glycosylation after settlement that could facilitate or regulate these metamorphic transitions. We conclude that the extent of protein glycosylation depends on the interspecific differences in the physiological and behavioral status of the invertebrate larvae.

Commonly Glycosylated Metabolism and Oxidative Stress Proteins Regulate Larval Metamorphosis

It is striking that many glycoproteins identified in this study are related to metabolic processes such as motility, cell differentiation, signal transduction, metabolism and oxidative stress. We suspect that larval metabolism becomes highly active during competency and early metamorphosis because the larvae require extra energy supplies to initiate and fuel the transition to the juvenile stage. It was reported that nonfeeding larvae continuously lose larval structures, and in their continuous search for habitats, they could generate enormous amounts of cellular stress.[33] It is reasonable to postulate that to counterbalance and/or reduce the stress and to facilitate speedy metamorphosis, a large amount of oxidative proteins and energy metabolism proteins are continuously synthesized and modified. On the other hand, oxidative stress proteins influence larval attachment and metamorphosis in response to environmental, chemical, and physical stressors.[34] The higher expression and glycosylation of energy metabolism proteins imply the activation of energy-producing pathways in the early metamorphosis stage.[35]

Another interesting observation was several differentially expressed glycosylated proteins were commonly found among the species at the same developmental stages (e.g., CL and JU) because glycosylation profiles change depending on the nature of the developmental stage. This implies that marine invertebrates share common metamorphic transitions, such as competency and attachment, that are influenced by differential glycosylation during larval development.[13,36]

Protein Expression Level Does Not Always Complement Alterations in Glycosylation

Tubulin, the main filament of the cytoskeleton that modulates cell stability and shape, is a heterodimer of α- and β-tubulin. Two isoforms (α and β) of tubulin (Table 1, spots 1 and 2) exhibited different patterns of expression in *B. neritina* and *P. vexillosa*, indicating possible stage-specific glycosylation during development. The differential glycosylation may regulate cytoskeleton alterations including increased polymerization or depolymerization of microtubules that can lead to the loss of larval structures or the formation of juvenile structures.[37,38] The opposite trend in the glycosylation changes in the cytoskeleton and total protein expression in *P. vexillosa* suggested that the protein expression level does not always complement the alteration in the glycosylation level. Only the oligosaccharide chains (glycans) attached to the polypeptides of glycoproteins may have possibly changed. Furthermore, carbohydrate can make up from 1 to 80% of the total protein mass and can change the overall structure of the polypeptide. Further investigation on the polysaccharide structure dynamics of selected glycoproteins would yield valuable insights into the glycobiology of developmental processes.

Tropomyosin, an actin-binding protein regulating the actin mechanism in muscle contractions, exists in a large number of isoforms such as tropomyosin, myosin heavy chain, and myosin

dx.doi.org/10.1021/pr200982k | J. Proteome Res. 2012, 11, 1330–1340

light chain.[39] The appearance or disappearance of glycoprotein spots during early (in *P. vexillosa*) or late developmental (in *B. neritina*) stages suggests that this protein corresponds to a developmental stage-specific isoform. The above observations suggest that protein glycosylation may influence cell and tissue assembly and disassembly of cytoskeleton proteins that occur more frequently when larvae are attaining competency to settle and metamorphose.

Glycosylation of Heat Shock Proteins Contribute to Stress Tolerance

Among the stress-related proteins that showed glycosylation changes, the HSPs and 14-3-3 family proteins were dominant. In this study, they exhibited specific glycosylation patterns in competent larvae of *B. amphitrite* and *B. neritina*, respectively. The stress response of marine invertebrate larvae during attachment and metamorphosis may involve a distinct strategy.[40] For instance, barnacle cyprids specialize in attachment and many juvenile structures are generated before attachment and metamorphosis.[41] Considering that the barnacle cyprids 'active' habitat selection behavior, their larval attachment is also an active process involving the synthesis of many proteins with modifications.[42,29] The increase in HSP glycosylation might be due to external stimuli because food deprivation in nonfeeding larvae can stimulate HSP expression in the early stages of larval development.[43] Stress tolerance may be associated with selective glycosylation of certain proteins at specific developmental stages. The elevated levels of HSPs are necessary to mediate the damage caused by oxidative stress[44] followed by limited reduction in ATP synthesis (Table 1, spot 8 and Figure 5D). The most significant effect of these changes may result in severe down-regulation of energy metabolism proteins (as indicated by the decrease in the glycosylation of energy metabolism-related proteins during development; Table 1, spots 8−15).[45] Hence, it can be argued that the induction of HSP70 contributes to protection of the cell from damage caused by stress. Given the above considerations, the elevated expression of HSPs together with 14-3-3 proteins may be caused by starvation of the larvae during the transition from larval stage to the juvenile stage.[46]

Energy Balance of Glycosylation Regulation of Metabolism and Stress-Related Proteins

The precise mechanism by which the increase or decrease of glycosylation mediates the activity of these proteins remains unidentified. Nevertheless, the observed glycosylation of the fatty acid metabolism-related proteins (EP1 and LDL receptor) in *P. vexillosa* suggests the possibility that oxidative stress induces shifts in fatty acid and/or ATP turnover. The above observation also suggests that specific glycosylation and the extent of modification are species- and developmental-stage specific. For example, the energy metabolism-related glycoproteins (14-3-3 and PDI) in *B. neritina* showed no significant changes during development except for vitellogenins. Furthermore, these proteins were not even glycosylated during *P. vexillosa* larval development. These selective changes in glycosylation could indeed reflect a physiological mechanism mediated by specific protein modification during the developmental process in marine invertebrates. Together with the observations presented here, the dynamics of protein modification and their expression provide overlapping, or complementary levels of regulation in cellular functions.[47,48] A common response to stress in marine invertebrates larvae is metabolic repression.[49,50] The results of the current study support the above observation that down-regulation of genes was related to energy metabolism (in this case, ATP2, CAL in *B. amphitrite* and VTG in *B. neritina*). It has been estimated that protein translation alone could consume up to 50% of cellular energy.[51] By suppressing energy metabolism through down-regulating the expression of relevant proteins, the energy can then be allocated to synthesize stress response proteins.[52] Perhaps this shift in energy usage was the result of a need to fuel the expression and glycosylation of fatty acid metabolism-related proteins such as EP1 and LDL receptors during the early developmental stages (PC and CL) in *P. vexillosa*. It could be argued that the glycosylation dynamics of given proteins under oxidative stress hampers the energy-related metabolic pathways for replacing essential cellular macromolecules during larval development. Sensory nervous system proteins expected to be important in larval metamorphosis.[13] Practical limitations in 2-DE proteomics approaches limit the detection and identification of low copy proteins in marine invertebrates. However, using a combination of shotgun LC−MS/MS approaches with sample prefractionation methods may allow possible identification of sensory/nervous system proteins.

■ CONCLUSIONS

To our knowledge, this is the first comparative study of the glycoproteome in different marine species. Using a combination of multiplex 2-DE and MS, we demonstrated substantial changes in protein glycosylation patterns during the larval to juvenile transition in *B. amphitrite*, *B. neritina*, and *P. vexillosa*. In addition, we identified 19 glycoproteins. Of these, 11 were differentially glycosylated and commonly expressed in *B. amphitrite* and *B. neritina*. Despite the strong similarities in glycoprotein patterns (i.e., identification of commonly glycosylated proteins in all three species), equally vast differences in protein expression and glycosylation ratios among the three species were observed. Possibly, these species used somewhat different mechanisms to complete their larval−juvenile transitions. On the basis of the results, we predict that marine larvae respond to oxidative stress and shifts in energy balances by changing their protein modification patterns (in this case, through protein glycosylation). However, deciphering biosynthesis patterns and functions in glycoproteins in marine invertebrates remains a major challenge because of the limited molecular information available. Our findings highlight the need for comprehensive analysis of glycoprotein structures and specific glycosylation sites that should ultimately result in a better understanding of glycoproteome dynamics during larval development in marine invertebrates.

■ AUTHOR INFORMATION

Corresponding Author

*Tel.: 0852-2358-733. Fax: 0852-2358-1559. E-mail: boqianpy@ust.hk.

■ ACKNOWLEDGMENTS

The authors thank Dr. Flora S. Y. Mok for her help in collecting *P. vexillosa* larvae, Dr. Kiyotaka Matsumura for his critical review of the manuscript, and Cherry Kwan for proof-reading the manuscript. This study was supported by an award from King Abdullah University of Science and Technology (SA-C0040/UK-C0016) and a grant from the Research Grants Council of the Hong Kong Special Administrative Region (AoE/P-04/04-II) to P.-Y. Qian.

ABBREVIATIONS:

CC, competent cyprids; AC, attached cyprids; JU, juvenile; CL, competent larvae; AL, attached larvae; PC, precompetent larvae; NU, nuplius; TUB, tubulins; ACT, actins; TM, tropomyosin or myosin light chain; hsp70, heat shock protein-70; HSP-hsp90, heat shock protein-70; 14-3-3, 14-3-3 zeta; ATPsyn-β, ATP synthase beta subunit; PDI, protein disulfide isomerase; MDH, mitochondrial malate dehydrogenase; CP, cathepsin L; CAL, calreticulin; CP3, cuticular protein 3; TCTP, translationally controlled tumor protein; VTG 6, vitellogenin-6; GALM, galactose mutarotase; EP1, enolase-phosphatase E1; CIF, cytoplasmic intermediate filament; LDLR, low-density lipoprotein receptor

REFERENCES

(1) Degnan, S. M.; Degnan, B. M. The initiation of metamorphosis as an ancient polyphenic trait and its role in metazoan life-cycle evolution. *Philos. Trans. R. Soc., B* **2010**, *365*, 641−651.

(2) Bishop, C. D.; Huggett, M. J.; Heyland, A.; Hodin, J.; Brandhorst, B. P. Interspecific variation in metamorphic competence in marine invertebrates: The significance for comparative investigations into the timing of metamorphosis. *Integr. Comp. Biol.* **2006**, *46* (6), 662−82.

(3) Hadfield, M. G.; Strathmann, M. F. Variability, flexibility and plasticity in life histories of marine invertebrates. *Oceanol. Acta* **1996**, *19*, 323−334.

(4) Degnan, B. M.; Souter, D.; Degnan, S. M; Long, S. C. Induction of metamorphosis in larvae of the ascidian *Herdmania momus* with potassium ions requires attainment of competence and an anterior signaling center. *Dev. Genes Evol.* **1997**, *206*, 370−376.

(5) Todd, C. D.; Lambert, W. J.; Thorpe, J. P. The genetic structure of intertidal populations of two species of nudibranch molluscs with planktotrophic and pelagic lecithotrophic larval stages: Are pelagic larvae 'for' dispersal? *J. Exp. Mar. Biol. Ecol.* **1998**, *228*, 1−28.

(6) Williams, E. A.; Craigie, A.; Yeates, A.; Degnan, S. M. Articulated coralline algae of the genus Amphiroa are highly effective natural inducers of settlement in the tropical abalone Haliotis asinina. *Biol. Bull.* **2008**, *215*, 98−107.

(7) Strathmann, R. R. Hypotheses on the origins of marine larvae. *Annu. Rev. Ecol. Syst.* **1993**, *24*, 89−117.

(8) Triyagarajan, V.; Pechenik, J. A.; Gosselin, L.; Qian, P. Y. Juvenile growth in barnacles: Combined effect of delayed metamorphosis and sub-lethal exposure of cyprids to low salinity stress. *Mar. Ecol.: Prog. Ser.* **2007**, *344*, 173−184.

(9) Thiyagarajan, V.; Hung, O. S.; Chiu, M. Y.; Wu, R. S. S.; Qian, P. Y. Growth and survival of juvenile barnacle *Balanus amphitrite*: Interactive effects of cyprid energy reserve and habitat. *Mar. Ecol.: Prog. Ser.* **2005**, *299*, 229−237.

(10) Scheer, B. T. The development of marine fouling communities. *Biol. Bull.* **1945**, *89*, 103−121.

(11) Woollacott, R. M.; Zimmer, R. L. Attachment and metamorphosis of the cheilo- ctenostome bryozoan *Bugula neritina* (Linne). *J. Morphol.* **1971**, *134*, 351−382.

(12) Mok, F.; Thiyagarajan, V.; Qian, P. Y. Larval development and metamorphic behaviour of subtropical spionid polychaete *Pseudopolydora vexillosa*. *J. Exp. Mar. Biol. Ecol* **2008**, *357*, 99−108.

(13) Heyland, A.; Moroz, L. L. Signaling mechanisms underlying metamorphic transitions in animals. *Integr. Comp. Biol.* **2006**, *46* (6), 743−759.

(14) Zhou, H.; Liu, Y.; Chui, J.; Guo, K.; Shun, Q.; Lu, W.; Jin, H.; Wei, L.; Yang, P. Investigation on glycosylation patterns of proteins from human liver cancer cell lines based on the multiplexed proteomics technology. *Arch. Biochem. Biophys.* **2007**, *459* (1), 70−78.

(15) Vandenborre, G.; Smagghe, G.; Ghesquière, B.; Menschaert, G.; Nagender Rao, R.; Gevaert, K.; Van Damme, E. J. Diversity in protein glycosylation among insect species. *PLoS ONE* **2011**, *23* (6), e16682.

(16) Acar, M.; Jafar-Nejad, H.; Takeuchi, H.; Rajan, A.; Ibrani, D.; Rana, N. A.; Pan, H.; Haltiwanger, R. S.; Bellen, H. J. Rumi is a CAP10 domain glycosyltransferase that modifies Notch and is required for Notch signaling. *Cell* **2008**, *132*, 247−258.

(17) Zhang, L.; Zhang, Y.; Ten Hagen, K. G. A mucin-type *O*-glycosyltransferase modulates cell adhesion during Drosophila development. *J. Biol. Chem.* **2008**, *283*, 34076−34086.

(18) Jensen, O. N. Interpreting the protein language using proteomics. *Nat. Rev. Mol. Cell Biol.* **2006**, *7* (6), 391−403.

(19) Yano, H.; Yamamoto-Hino, M.; Goto, S. Spatial and temporal regulation of glycosylation during Drosophila eye development. *Cell Tissue Res.* **2009**, *336*, 137−147.

(20) Thiyagarajan, V.; Harder, T.; Qiu, J. W.; Qian, P. Y. Energy content at metamorphosis and growth rate of the juvenile barnacle *Balanus amphitrite*. *Mar. Biol.* **2003**, *143* (3), 543−554.

(21) Thiyagarajan, V.; Harder, T.; Qian, P. Y. Relationship between cyprid energy reserves and metamorphosis in the barnacle *Balanus amphitrite* Darwin (Cirripedia; Thoracica). *J. Exp. Mar. Biol. Ecol.* **2002**, *280* (1−2), 79−93.

(22) Wong, Y. H.; Arellano, S. M.; Zhang, H.; Ravasi, T.; Qian, P. Y. Dependency on *de novo* protein synthesis and proteomic changes during metamorphosis of the marine bryozoan *Bugula neritina*. *Proteome Sci.* **2010**, *8*, 25.

(23) Chandramouli, K. H.; Mok, F. S.; Wang, H.; Qian, P. Y. Phosphoproteome analysis during larval development and metamorphosis in the spionid polychaete *Pseudopolydora vexillosa*. *BMC Dev. Biol.* **2011**, *25* (11), 31.

(24) Ramagli, L. S.; Rodriguez, L. V. Quantitation of microgram amounts of protein in two-dimensional polyacrylamide gel electrophoresis sample buffer. *Electrophoresis* **1985**, *6*, 559−563.

(25) Zhang, Y.; Sun, J.; Xiao, K.; Arellano, S. M.; Thiyagarajan, V.; Qian, P. Y. 2D gel-based multiplexed proteomic analysis during aarval development and metamorphosis of the biofouling polychaete tubeworm *Hydroides elegans*. *J. Proteome Res.* **2010**, *9* (9), 4851−4860.

(26) Thiyagarajan, V.; Wong, T.; Qian, P. Y. 2D gel-based proteome and phosphoproteome analysis during larval metamorphosis in two major marine biofouling invertebrates. *J. Proteome Res.* **2009**, *8* (6), 2708−2719.

(27) Qian, P. Y.; Wong, T. H.; Zhang, Y. Changes in the proteome and phosphoproteome expression in the bryozoan *Bugula neritina* larvae in response to the antifouling agent butenolide. *Proteomics* **2010**, *10*, 1−12.

(28) Zhang, H.; Wong, Y. H.; Wang, H.; Chen, Z.; Arellano, S. M.; Ravasi, T.; Qian, P. Y. Quantitative proteomics identify molecular targets that are crucial in larval settlement and metamorphosis of *Bugula neritina*. *J. Proteome Res.* **2011**, *7* (10), 349−60.

(29) Zhang, Y.; Xu, Y.; Arellano, S. M.; Thiyagarajan, V.; Qian, P. Y. Comparative proteome and phosphoproteome analyses during cyprid development of the barnacle *Balanus* (=*Amphibalanus*) *amphitrite*. *J. Proteome Res.* **2010**, *9* (6), 3146−3157.

(30) Kenneth, J. L.; Thomas, D. S. Analysis of relative gene expression data using real-time quantitative PCR and the 2-CT method. *Methods* **2001**, *25*, 402−408.

(31) Qiu, J. W.; Qian, P. Y. Effects of food availability, larval source and culture method on larval development of *Balanus amphitrite Amphitrite* Darwin: Implications for experimental design. *J. Exp. Mar. Biol. Ecol.* **1997**, *217*, 47−61.

(32) Pechenik, J. A. On the advantages and disadvantages of larval stages in benthic marine invertebrate life cycles. *Mar. Ecol.: Prog. Ser.* **1999**, *177*, 269−297.

(33) Rueda-Jasso, R.; Conceicao, L. E. C.; Dias, J.; De Coen, W.; Gomes, E.; Rees, J. F.; Soares, F.; Dinis, M. T.; Sorgeloos, P. Effect of dietary non-protein energy levels on condition and oxidative status of Senegalese sole (*Solea senegalensis*) juveniles. *Aquaculture* **2004**, *231*, 417−433.

(34) Tomanek, L. Environmental proteomics: Changes in the proteome of marine organisms in response to environmental stress, pollutants, infection, symbiosis, and development. *Ann. Rev. Mar. Sci.* **2011**, *3*, 373−399.

(35) Guidugli, K. R.; Piulachs, M. D.; BelléS, X.; LourençO, A. P.; Simões, Z. L. Vitellogenin expression in queen ovaries and in larvae of

both sexes of *Apis mellifera*. *Arch. Insect Biochem. Physiol.* **2005**, *59*, 211−218.
(36) Hadfield, M. G. Why and how marine invertebrate larvae metamorphose so fast. *Semin. Cell Dev. Biol.* **2000**, *11*, 437−443.
(37) Chandramouli, K. H.; Lisa, S.; Qian, P. Y. Proteome and phosphoproteome analysis during larval development in polychaete *Capitella sp. I. Proteome Sci.* **2011**, *9*, 51.
(38) Hammond, J. W.; Cai, D.; Verhey, K. J. Tubulin modifications and their cellular functions. *Curr. Opin. Cell Biol.* **2008**, *20* (1), 71−76.
(39) Mizuno, H.; Hamada, A.; Shimada, K.; Honda, H. Tropomyosin as a regulator of the sliding movement of actin filaments. *Biosystems* **2007**, *90* (2), 449−55.
(40) Kelvin, K. W.; Ackley, C. L.; Priscilla, T. Y.; Thiyagarajan, V. Response of larval barnacle proteome to CO2-driven seawater acidification. *Comp. Biochem. Physiol., Part D: Genomics Proteomics* **2011**, *6* (3), 310−321.
(41) Hadfield, M. G.; Carpizo-Ituarte, E. J.; del Carmen, K.; Nedved, B. T. Metamorphic competence, a major adaptive convergence in marine invertebrate larvae. *Integr. Comp. Biol.* **2001**, *41*, 1123.
(42) Thiyagarajan, V.; Qian, P. Y. Proteomic analysis of larvae during development, attachment, and metamorphosis in the fouling barnacle, *Balanus amphitrite*. *Proteomics* **2008**, *8*, 3164−3172.
(43) Monari, M.; Foschi, J.; Rosmini, R.; Marin, M. G.; Serrazanetti, G. P. Heat shock protein 70 response to physical and chemical stress in *Chamelea gallina*. *J. Exp. Mar. Biol. Ecol.* **2011**, *397*, 71−78.
(44) Podrabsky, J. E.; Somero, G. N. An inducible 70 kDa-class heat shock protein is constitutively expressed during early development and diapause in the annual killifish *Austrofundulus limnaeus*. *Cell Stress Chaperones* **2007**, *12* (3), 199−204.
(45) Silverman-Gavrila, L. B.; Senzel, A. G.; Charlton, M. P.; Feng, Z. P. Expression, phosphorylation, and glycosylation of CNS proteins in aversive operant conditioning associated memory in Lymnaea stagnalis. *Neuroscience* **2011**, *186*, 94−109.
(46) Kjørsvik, E.; Pittman, K.; Pavlov, D. From fertilisation to the end of metamorphosis. Functional development. In *Culture of Cold-Water Marine Fish*;Moksness, E., Kjørsvik, E., Olsen, Y., Eds.; Blackwell Publishing Ltd: Oxford, U. K.,2004; p 204−278.
(47) Scroggins, B. T.; Neckers, L. Post-translational modification of heat-shock protein 90: impact on chaperone function. *Expert Opin. Drug Discovery* **2007**, *2*, 1403−1414.
(48) Tomanek, L.; Zuzow, M. J.; Ivanina, A. V.; Beniash, E.; Sokolova, I. M. Proteomic response to elevated pCO2 level in eastern oysters, *Crassostrea virginica*: Evidence for oxidative stress. *J. Exp. Biol.* **2011**, *214*, 1836−1844.
(49) Rosa, R.; Seibel, B. A. Synergistic effects of climate-related variables suggest future physiological impairment in a top oceanic predator. *Proc. Nat. Acad. Sci. U. S. A.* **2008**, *105*, 20776−20780.
(50) Nakamura, M.; Ohki, S.; Suzuki, A.; Sakai, K. Coral larvae under ocean acidification: Survival, metabolism, and metamorphosis. *PloS ONE* **2011**, *6*, e14521.
(51) Holcik, M.; Sonenberg, N. Translational control in stress and apoptosis. *Nat. Rev. Mol. Cell Biol.* **2005**, *6*, 318−327.
(52) Place, S. P.; O'Donnell, M. J.; Hofmann, G. E. Gene expression in the intertidal mussel *Mytilus californianus*: Physiological response to environmental factors on a biogeographic scale. *Mar. Ecol.: Prog. Ser.* **2008**, *356*, 1−14.